Searching for CO_2 in marine sediment pore waters: Methods and detection limits using laser Raman spectroscopy

Anna Gallagher, Carleton College

Mentors: Peter G. Brewer, Edward T. Peltzer, and Peter M. Walz

Summer 2012

Keywords: Raman spectroscopy, carbon dioxide, pore waters, in situ, DORISS II

ABSTRACT

Marine sediment pore waters are of interest due to the many significant natural chemical processes occurring in them as well as for possible applications to carbon dioxide sequestration as a method of lowering greenhouse gas emissions. This paper examines methods of detecting CO_2 in pore waters together with the other major components of the standard diagenetic sequence (CH_4, SO_4, H_2S) so as to evaluate means of distinguishing natural versus non-diagenetic intrusions of dissolved CO_2 (e.g. manmade or volcanic). We also evaluate the potential and limitations of our current DORISS II seagoing Raman system for this purpose. We have tested in the laboratory methods for in situ observations and experiments with the DORISS II system, and we have estimated the dissolved CO_2 detection limit. We show that it should be fully capable of measuring CO_2 levels typically found in mildly reduced sediment pore waters (~ 8 mM), provided that the system is equipped with a microliter acid delivery system to lower the pH of the sample fluid to pH 4 or below thus converting HCO3 to the spectroscopically favored CO2 form immediately prior to spectral collection.

INTRODUCTION

The spectroscopic study of chemistry occurring in marine sediment pore waters has historically been limited by a lack of technology to perform in situ measurements and to successfully filter out strong fluorescent signals produced by sediment particles [Zhang et al, 2012]. However, through recent advances in engineering at the Monterey Bay Aquarium Research Institute (MBARI), particularly the development of the DORISS II (Deep-Ocean Raman In Situ Spectrometer) system and its pore water probe attachment, it is now possible to construct detailed chemical profiles up to 50 cm into the sediment. This has paved the way for a greater understanding of the diagenetic processes taking place on the sub-seafloor, as well as unique phenomena that affect the mass balance of those processes, than ever before.

It is well known that typical background dissolved sulfate levels in seawater are close to 28 mM and that this concentration may be reduced to zero in strongly reducing sediments where microbial oxidation of methane is occurring [Reeburgh, 2007]. Zhang et al. [2011] also showed through direct measurement of methane in situ that the two decrease proportionally to each other, in accordance with the following anaerobic oxidation:

$$CH_4 + SO_4^{2-} \rightarrow HCO_3^- + HS^- + H_2O$$

However, monitoring of this reaction and other similarly significant ones occurring in sediment pore waters has thus far only been carried out through measurement of the disappearance of the reactants rather than the appearance of products. The concentration of dissolved sulfide can be determined spectroscopically and the separate H2S and HS- species resolved, but detection of dissolved HCO3- remains a challenge due the weak Raman cross section of this species.

The bicarbonate ion is a poor Raman scatterer, though under lowered pH conditions it is readily transformed into the dissolved CO2 form.

$$HCO_3^- + H^+ \rightleftharpoons H_2CO_3 \rightleftharpoons CO_2 + H_2O$$

The symmetrical CO_2 molecule produces a considerably stronger Raman signal, so with a reliable method of acidifying pore water samples prior to Raman measurement, our capacity for more closely examining the diagenetic sequence in pore waters would be greatly enhanced.

Additionally, proposals in recent years for ocean carbon dioxide sequestration as a means of reducing greenhouse gas emissions have led to extensive feasibility studies on the topic. Though initial experiments involving the formation of CO_2 hydrate structures on the seafloor were not promising due to a number of factors [Brewer, 2007; D.L. Thistle et al., 2007], it remains to be seen if CO_2 storage in the sub-seafloor is an option. In practice the Norwegian Sleipner project has already carried out active CO_2 storage in deep sandstone aquifers under the North Sea on the million ton scale.

The focus of the project described here was to assess the CO_2 detection capabilities of the DORISS II. Additionally, MBARI's seagoing system, operated by the Brewer team, was compared with its laboratory Raman laser system in order to predict what, if any, spectral differences there are between preparatory lab experiments and in situ measurements. Experiments were carried out with the aim of optimizing upcoming research cruises in fall 2012 that will be making use of the DORISS II system to observe carbon dioxide in deep-sea sediment pore waters. It should be noted that the success of these experiments also hinges on the completion of a system to deliver phosphoric acid directly to the Raman cell to acidify seawater samples immediately prior to spectral collection. A preliminary version of the system is already in place, though it has yet to be tested in situ.

Previous experiments assessing the capabilities of DORISS I to detect CO_2 in seawater yielded a limit estimation of ~10 mM [Dunk et al., 2005]. However, these experiments were all conducted in a carefully controlled CO_2-enriched seawater system and the reported limit was calculated rather than observed. Our hope was to establish a similar estimate of the DORISS II limit through more direct means. Though it would be ideal to have the ability to measure background CO_2 levels (2.2 mM), our primary aim is to monitor sediment pore waters, which, when affected only by the mass balance of microbial oxidation reactions, reach their maximum around 30 mM (28 mM SO_4^{2-} + 2 mM background CO_2).

MATERIALS AND METHODS

LASER RAMAN SYSTEMS.

Two Raman systems were examined over the course of the experiments: the onshore laboratory set-up and the second-generation deep-ocean Raman in situ spectrometer (DORISS II) seagoing system [Zhang, 2012]. Both laser Raman RXN optical bench f/1.8i spectrometers are products of Kaiser Optical Systems, Inc. (KOSI). Each system consists of a spectrometer, an optic, a 532-nm Nd:YAG laser with a spectral range of 100 to 4000 cm^{-1}, and front-illuminated cooled 2048 x 512 CCD camera (Andor technology) with a duplex grating that splits the spectrum on the CCD chip's face, yielding a digital resolution of ~2 Δcm^{-1}.

Laboratory system (Figure 1a): The benchtop instrument consists of a Coherent model DPSS 532 laser and an NCO-1.3-VIS optic with ~38 mW of laser power at the probehead. CO_2 solubility tests were carried out in a high-pressure, low-temperature hydrate Raman cell made by S.O. Colgate, Inc (cell volume: 1 cc) with front viewport and rear illumination single-crystal sapphire windows. For complete set-up, refer to Figure 1a.

DORISS II system (Figure 1b): KOSI developed this seagoing Raman instrument by modifying the design of the DORISS I as requested by the Brewer team based on observations of the original system [Zhang et al, 2012]. It uses a KOSI Invictus laser and its delivery through the 6.3-mm diameter immersion optic, which was used throughout the experiments described here, yields ~58 mW of laser power at the probehead. The team has also developed a 35-cm probe for extraction of pore fluids from surrounding sediment [Zhang et al., 2010] in the sub-seafloor region. The probe contains a 10-μm frit through which the sample liquid enters, is drawn up through a 2-mm passage, and released into the optical cell containing a sapphire window for Raman measurement. For complete set-up, refer to Figure 1b.

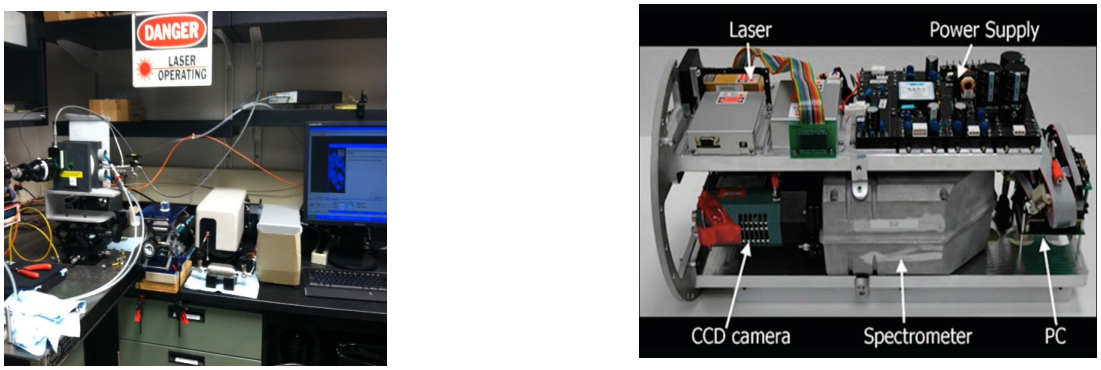

(a) (b)

Figure 1. Complete set-ups for (a) the laboratory Raman system and (b) the DORISS II system [photo source: Zhang et al., 2012].

Both lasers were calibrated immediately prior to spectral collection; neon and tungsten lamps were used for wavelength and intensity calibrations, respectively. The laser wavelength itself was calibrated to the 801 cm^{-1} Raman line of cyclohexane. Calibration and sample spectra were collected with KOSI's HoloGRAMS software with dark spectrum subtraction and wavelength/intensity corrections applied before saving in generic spectrum (.spc) format.

LABORATORY SET-UP.

There were three major experimental phases: a series of high-pressure CO_2 solubility tests using the benchtop optic and pressure cell; a comparison of the sensitivity of the two Raman systems using varied optics and optical paths; and an estimation of the detection limit of CO_2 using the DORISS II system. Each phase had a unique set up, which will be described in detail here.

CO_2 solubility tests: A temperature-controlled water bath was connected to the Raman pressure cell via plastic tubing that circulated water to the area surrounding the cell while a digital thermometer monitored the temperature within it. The evacuated cell was filled approximately halfway with seawater that had been pre-acidified to pH 3.8 using a stock solution of 70% H_3PO_4. A stainless steel cylinder containing the gas to be equilibrated in the seawater, either pure CO_2 or a 75% N_2/25% CO_2 mix, was connected to the pressure cell. Gas was subsequently released into the cell until it reached the

desired pressure. The gas/seawater mixture was allowed to equilibrate for ~60 minutes prior to collection of the Raman spectrum. Between four and seven equilibrations were performed at varying pressures ranging from 25 to 800 psig at each cell temperature (5, 10, 20, and 30°C) using the pure CO_2 cylinder; then, five equilibrations were carried out between 100 and 800 psig using the mixed N_2/CO_2 cylinder at 20°C.

Raman systems sensitivity comparison: A Raman spectrum was collected for several sodium sulfate solutions of known concentrations (5, 15, 25, 35, 45, and 55 mM) at room temperature and 1 atm using each of four different optical set ups: benchtop Raman system, optic focused in the pressure cell containing Na_2SO_4 solution to be analyzed; benchtop Raman system, open optic focused directly in Na_2SO_4 solution contained in a plastic bottle; DORISS II Raman system, open optic focused directly in Na_2SO_4 solution in a plastic bottle; and, DORISS II Raman system with 35-cm pore water probe tip attached to the optic, probe tip immersed in solution. See Figure 2a-2d.

CO_2 Raman detection limit investigation: Using a pressure regulator, CO_2-containing gas was released from a steel cylinder into a beaker containing acidified seawater at 1 atm pressure and sealed with parafilm. Gas was bubbled into the beaker for ~30 minutes to saturate the fluid, at which point the 6.3-mm DORISS optic was immersed in the solution and Raman spectra of the water phase were collected. The procedure was carried out using both pure CO_2 and 75% N_2/25% CO_2. Several spectra were collected for each sample using varied exposure times and number of accumulations with the aim of obtaining the most visible peaks possible for analysis.

MODIFIED HENRY'S LAW SOLUBILITY CALCULATIONS.

The CO_2 solubility tests at varying temperatures required us to convert the pressure of gas released into the cell to a concentration of dissolved CO_2, in molar terms, to obtain a meaningful interpretation of the spectral data. We used a modified Henry's law equation presented by Weiss [1974] that is relevant to nonideal gases for this conversion. The equations used for pure CO_2 gas versus mixed N_2/CO_2 differ slightly because the fugacity, or apparent pressure, will not be the same in a multi-component gas system as in a pure gas system.

Both systems do, however, use the same basic equation as a starting point, a variation of Henry's law:

(1) $$[CO_2] = K_0 f_{CO_2} \exp\left[(1-P)\bar{v}_{CO_2} / RT\right]$$

Where K_0 is the solubility coefficient; f_{CO_2} is the fugacity of CO_2 (atm); P is pressure (atm); ν_{CO_2} is the partial molal volume of CO_2 in solution (32.3 cm^3/mol, in our tests); R is the gas constant (82.05746 cm^3*atm/K*mol); and T is temperature (K).

While the other terms are known, the solubility and fugacity terms require further calculation. K_0 varies with temperature and is equal to the Bunsen coefficient (the volume of gas that is absorbed per unit volume of solution, when total pressure = fugacity = 1 atm) per unit volume of one mole of gas at STP. The formula for solubility is as follows:

(2) $$\ln K_0 = A_1 + A_2(100/T) + A_3 \ln(T/100) + S‰[B_1 + B_2(T/100) + B_3(T/100)^2]$$

Where the A's and B's are constants[1], T is temperature (K), and S‰ is salinity (parts per thousand, ~32.5 for the seawater used in all of our experiments) [Weiss, 1974]. This holds true for both the pure gas and mixed gas.

CO_2 fugacities for the pure CO_2 and N_2/CO_2 mix were calculated using the virial equation of state. According to Weiss, the equations of state for pure substances and for mixtures as presented in Benedict et al., 1940 and Benedict et al., 1942, respectively, should be used at pressures >10 atm, but this difference was negligible compared to the error introduced during Raman spectral collection and analysis, so we used the much simpler virial equation of state for our solubility calculations [Zeebe, 2001]. The equations are quite similar; the main difference is that the mixed gas equation includes extra terms that better represent a multi-component system. Weiss's 1974 paper does not account for water vapor pressure in his equations, but we have included it in our own calculations for the sake of completeness [Weiss et al., 1980]:

(3) $$\ln(f_{CO_2} / P_{CO_2}) = P_{total} \times B(T)/RT$$

(4) $$\ln(f_{CO_2} / P_{CO_2}) = P_{total} \times [B(T) + 2\delta]/RT$$

[1] For mols/L calculations: A_1 = -58.0931, A_2 = 90.5069, A_3 = 22.2940, B_1 = 0.027766, B_2 = -0.025888, B_3 = 0.0050578; for mols/kg calculations: A_1 = -60.2409, A_2 = 93.4517, A_3 = 23.3585, B_1 = 0.023517, B_2 = -0.023656, B_3 = 0.0047036 (Weiss, 1970)

In equation 3 for the pure gas case, P_{CO2} is simply the difference of the total pressure in the system (P_{total}) and the vapor pressure of water ($P_{vap,H2O}$).[2] In equation 4 for the case of CO2 in air, P_{CO2} is the same difference multiplied by the mole fraction of CO_2 in dry air (~0.25, equivalent to 250,000 ppm). In both equations, B(T) is second virial coefficient[3] (carrying the expansion out beyond this coefficient has an insignificant effect on the calculations); in equation 10, δ is the cross virial coefficient[4] (accounting for interactions between CO_2 and air).

With these two coefficients settled, we can apply the conditions of each of our experiments to calculate the concentration of CO_2 dissolved in the acidified seawater in our cell using equation 1. The equation was written into a Visual Basic script and subsequently solved for each set of experimental conditions in an Excel workbook.

SPECTRAL ANALYSIS.

After collection in the HoloGRAMS program, spectra were exported to GRAMS/AI (Thermo Electron Corp.) for analysis. Manual baseline corrections were performed in regions of the spectrum containing known peaks of interest (approximately 900-2000 cm-1). Peak identification, selection, and integration were completed using a peak-fitting tool that looks for both Gaussian and Lorentzian distribution elements. The peak positions, heights, widths, fit parameters, and areas were then exported to Excel for further processing. Approximate Raman shifts (in cm-1) for peaks integrated in each set of experiments are listed below.

CO_2 solubility: 1275 (CO_2 bend), 1383 (CO_2 stretch), 1640 (H_2O bend)

Systems sensitivity comparison: 981 (SO_4^{2-} stretch), 1640 (H_2O bend)

CO_2 detection limit: 1275 (CO_2 bend), 1383 (CO_2 stretch), 1640 (H_2O bend)

Note that the injection of phosphoric acid prior to spectral collection may cause peak formation at shifts corresponding to H_3PO_4 (~892 cm^{-1}) and $H_2PO_4^-$ (~872 cm^{-1} and ~1074 cm^{-1}) [Cherif et al., 2000]. However, if visible, these peaks would be spaced sufficiently far from other peaks of interest that they would not complicate our analysis.

---

[2] $\ln(P_{vap,H_2O}) = 24.4543 - (6745.09/T) - 4.8489\ln(T/100) - 0.000544$ (Weiss et al., 1980)

[3] $B(T) = -1636.75 + 12.0408T - 3.27957 \times 10^{-2}T^2 + 3.16528 \times 10^{-5}T^3$ (Weiss, 1974)

[4] $\delta_{CO_2-air} = 57.7 - 0.118T$ (Weiss, 1974)

The intensity of a Raman peak is directly proportional to, among other variables, the amount of the species it represents in a sample. This makes for a convenient method of determining concentrations of various compounds. Dunk et al. [2005] defines the intensity of Raman scattering using the following equation:

(5) $R = IKP\sigma C$

In which R = Raman peak area, I = laser intensity, K represent a set of instrument parameters (ie transmission, efficiency), P = path length, σ is the scattering efficiency of the compound (better scatterers will produce more intense peaks), and C = concentration per unit volume.

Fluctuations in a number of these variables can cause the peak area measurement to change unpredictably, so it is useful to have a compound present in the sample that can be used as an internal standard. Since the concentration of water in seawater remains essentially constant at ~55 M [Zhang et al., 2012] and its Raman signature is well understood, it was the ideal choice for an internal calibration tool in our experiments. All peaks were, therefore, normalized to the H_2O stretching band (~1640 cm^{-1}) in the following manner:

(6) $(R_i/R_{H_2O}) \times N = R_i^*$

In the above equation, R_{H_2O} is the Raman peak area of the H_2O stretching band, R_i is the area of the peak corresponding to compound *i*, N is an arbitrary integer, and R_i^* is the normalized peak area of compound *i*. Since, for a given spectrum, the parameters I, K, and P will be constant for all compounds represented by peaks, these terms would be in both the numerator and denominator using the same normalization technique, effectively cancelling each other out. That leaves us with:

(7) $R_i^* = \mathrm{N} \times (\sigma_i \mathrm{C}_i/\sigma_{H_2O}\mathrm{C}_{H_2O})$

The efficiency of scattering is intrinsic to a compound, so σ_i/σ_{H_2O} should be the same across all samples. So, the normalized peak area is directly proportional to the ratio of the concentrations of the water-to-target species. Since the water concentration also does not change (seawater is a constant 55 M H_2O), the relative Raman peak areas reflect the relative concentrations of a substance and this information can be used similarly to a Beer's law plot.

The areas of the individual peaks in the CO_2 Fermi dyad (Raman shifts 1275 and 1383 cm^{-1}), however, have been shown to deviate from this proportionality rule; the two peaks react differently with temperature and pressure variations, so equation 7 does not apply. However, their summed areas normalized to the water peak at 1640 cm^{-1} are consistently proportional to CO_2 concentration (Coward, 2011) and thus, we used this method for analysis.

RESULTS

CO_2 SOLUBILITY TESTS.

The raw spectra for the pure CO_2 at 30°C solubility set are overlaid and shown in Figure 2a; pressures in the Raman cell, in order of increasing peak intensity, are 100, 200, 400, 600, and 800 psig. Processed spectral data for the 30°C spectra, as well as those for 5, 10, and 20°C, were plotted and are shown in Figure 2b.

Concentrations increase with pressure and, in keeping with equation 7, the summed Raman peak areas of the Fermi dyad increase proportionally to CO_2 concentrations. The same basic analysis was also repeated for one set of spectra collected using a 75% N_2/25% CO_2 mixed gas at 20°C; this data set is also plotted in Figure 2b.

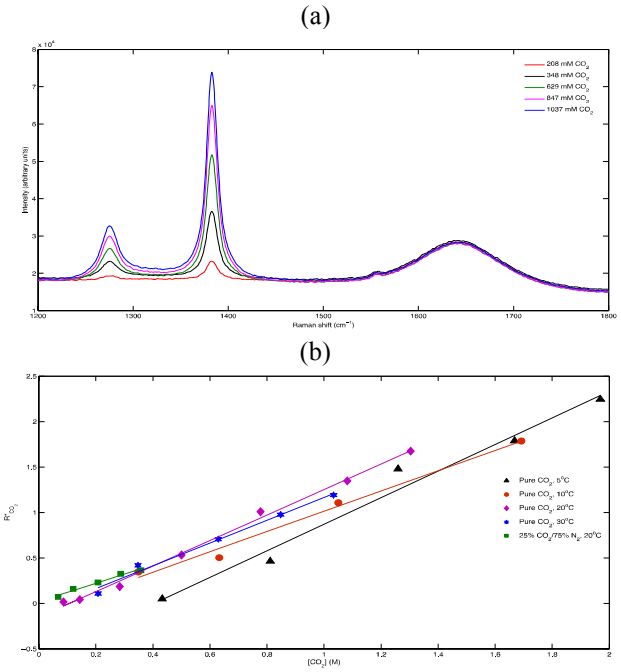

Figure 2. Overlaid Raman spectra of pure CO_2 at increasing pressures after equilibration with acidified seawater at 30°C (a) demonstrate peak area proportionality with species concentration. The spectra collected at all CO_2 pressures and temperatures of interest were processed in GRAMS and their CO_2 concentrations were calculated using the Henry's law equations presented in the Methods section. The normalized (N = 1) CO_2 peak area is plotted vs. concentration (b). Linear best-fit equations (5°C, pure CO_2 : 1.46x – 0.589; 10°C, pure CO_2: 1.12x – 0.104; 20°C, pure CO_2: 1.41x – 0.152; 30°C, pure CO_2: 1.26x – 0.090; 20°C, 75% N_2/25% CO_2: 1.00x + 0.021) were calculated using the polyfit function in MATLAB.

RAMAN SYSTEMS SENSITIVITY COMPARISON.

Visual inspection of the Raman spectra in HoloGRAMS as well as data output from the peak-fitting tool in GRAMS both indicate that the DORISS laser setups yield stronger signals than both of the benchtop system setups. Additionally, the two setups using the DORISS II laser yielded very similar results, as did the two setups using the laboratory optic. However, the difference between the two optics themselves was quite apparent (refer to Figure 3b). Based on this, it appears that the optic has a much larger effect than the optical path on signal intensity. The average signal ratio for the DORISS II system with pore water probe to benchtop system focused in pressure cell was 3.1 with a range of 2.6 to 3.9. The pressure cell does appear to lower signal intensity somewhat, as it was noticeably weaker than the open optic focused in the sodium sulfate solution.

When SO peaks were normalized to the water peak (N = 1), linear best-fit equations yielded very similar slopes for all four setups. For complete best-fit equations, refer to Figure 3c.

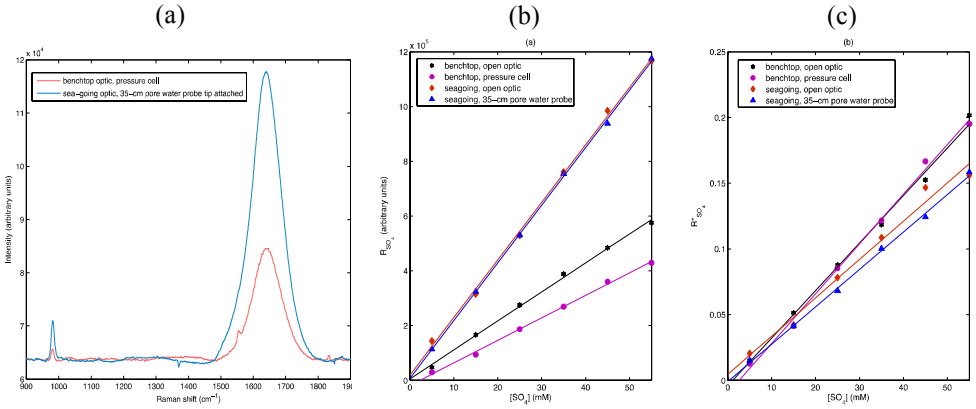

Figure 3. Results of Raman systems comparison using sodium sulfate standard solutions. The greater sensitivity of the seagoing system versus the laboratory system is exemplified by the overlaid 5-mM Na_2SO_4 spectra in (a); the raw peaks areas obtained from the DORISS II test are ~3.9x those of the benchtop pressure cell test. This is also evident in the raw data comparison of all four Raman setups (b), though once the sulfate peaks are normalized to water (c), approximately the same slope is obtained, as expected (benchtop, in cell: y = 0.0038x – 0.0097; benchtop, open optic: y = 0.0036x – 0.0041; DORISS II, open optic: 0.0029x + 0.0044; DORISS II with pore water probe: 0.0029x – 0.0010).

CO_2 RAMAN DETECTION LIMIT INVESTIGATION.

Using the modified Henry's law solubility rules, pure CO_2 (4a) at 14.7 psi and ~21°C yields a dissolved CO_2 concentration of 31.7 mM; 25% CO_2/75% N_2 gas mixture corresponds under the same conditions corresponds to a concentration of 7.95 mM. Due to the long total accumulation time for each spectrum that could resolve the peaks, it was only possible to collect one spectrum at each exposure/accumulation combination. However, it was expected that baseline noise and peak-fitting variability would be significant factors in the results obtained through spectral processing. Accordingly, each spectrum was processed three times in GRAMS to assess reproducibility at the two CO_2 concentrations. Normalized data for the three repeat correction/integrations series at each exposure/accumulations trial are plotted in Figure 4.

We could not discern an optimal exposure/accumulation parameter combination in either analysis of these plots or through visual inspection of the spectra themselves. However, as it was possible to integrate the peaks and obtain somewhat consistent results in the seawater spectrum containing 7.9 mM CO_2, we have estimated the CO_2 detection limit for the DORISS II system to be in the range of 7-8 mM. This estimate is based almost entirely on visual inspection of the spectra; as there was only one repeat of the saturation, there was no way to calculate the signal-to-noise ratio for the two Fermi dyad peaks. However, we cannot say with any confidence that we would be able to either notice or integrate a peak at 1275 cm^{-1} any smaller than those in the spectra we did obtain; it is on this fact that we base our estimate.

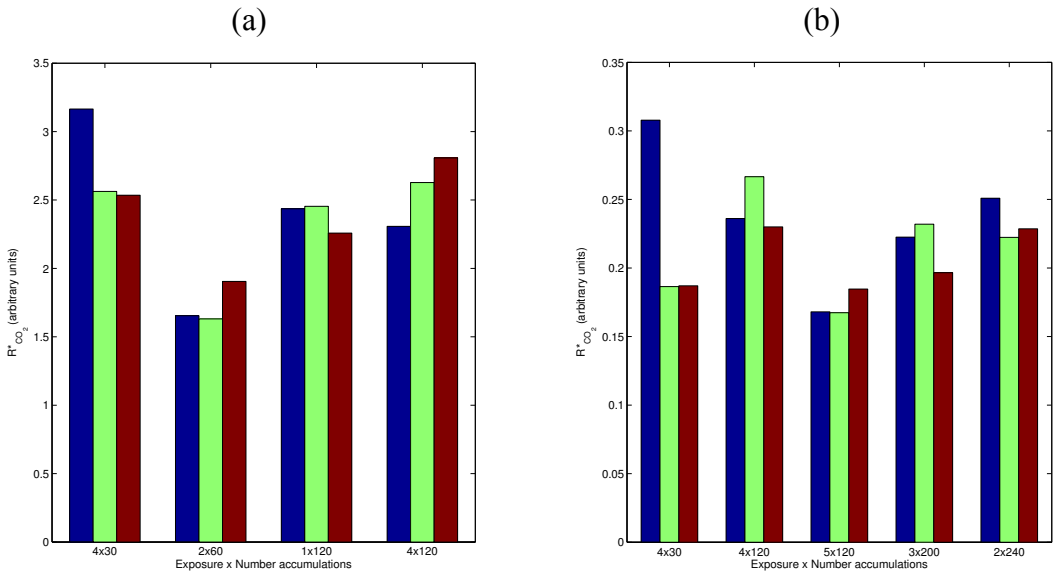

Figure 4. Normalized peak areas (N = 100) for repeat spectral baseline corrections and integrations in (a) pure CO_2 gas at 1 atm, 21°C and (b) mixed 75% N_2/25% CO_2 gas at 1 atm, 21°C.

DISCUSSION

The laboratory experiments just described have yielded information that will be valuable in the future, particularly as preparations for the fall 2012 cruise get underway. However, they have also illuminated aspects of the current Raman system that will need improvement if we are to make progress in the detection of CO_2 in sediment pore waters.

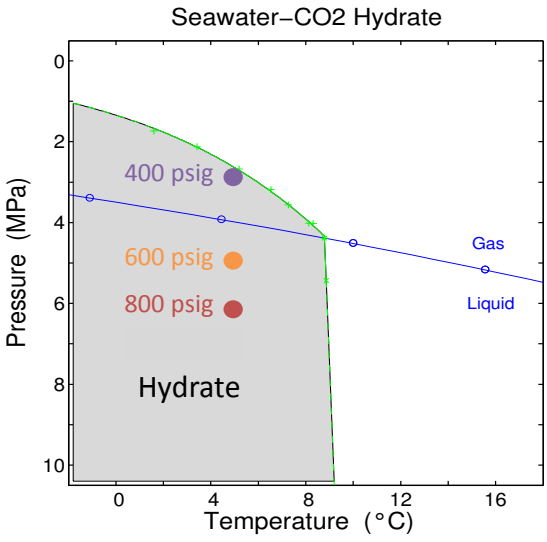

Figure 5. Phase diagram indicating the pressure-temperature conditions that favor hydrate formation. Pressure cell experiments carried out at 5°C with 600 and 800 psig CO_2 (represented with orange and red dots, respectively) simulate conditions that could well be observed in the deep ocean, where sub-seafloor CO_2 sequestration possibilities are being investigated.

First of all, it is evident in all three experiments that there are limitations to the accuracy of manual spectral processing. Though our baseline correction and peak-fitting routine is passable at higher CO_2 gas concentrations, attempting to quantify

lower concentrations of CO_2 (or any chemical species) at low concentrations introduces significant error due to a low signal-to-noise ratio. And, as is evident in plots presented in this paper of the CO_2 solubility experiments and the Raman systems comparison (Figures 2-3), the processing routine can cause issues even at higher pressures. All best-fit lines in both plots should, in theory, have the same slope and intercept (with the possible exception of the 5°C data, to be discussed below); though the slopes of normalized data are all similar to each other, they are certainly not identical. In the case of the data collected on CO_2 solubility at varied temperatures, the range of values is quite broad (slopes were calculated to be anywhere between 1.00 and 1.46 M^{-1}). And, in both experiments, it would be logical for the y-intercept to be close to zero, though this was not the case for the solubility experiments (background CO_2 levels in seawater may allow for a slight deviation, though this value is close enough to zero that the intercepts would be extremely close to zero). An improved spectral processing method could minimize these issues, as could a stronger Raman signal and reduced baseline noise.

Secondly, apart from quantifying the difference between the laboratory laser Raman and the DORISS II, the systems comparison made it clear that the detection limit of the laboratory laser focused in the pressure cell is significantly lower than that of the DORISS II. When analyzing spectra from the pure CO_2 gas equilibration in seawater at 25 psig (~86 mM), it became evident that we were nearing the detection limit for the species. Though the collection and analysis method could be improved upon in the future, the detection limit for this system will invariably be higher than that of the DORISS II. Thus, in-lab simulations of deep-ocean conditions may be limited if carried out in the HP-LT cell. Though not a deterrent to the continuation CO_2 pore water investigations, it is a factor to be considered when preparing a new set of in situ experiments.

And finally, it should be briefly noted that the 5°C data collected in the pressure cell has a substantially higher error than any of the other data sets. This could be due to a variety of factors, but one distinct possibility is occurrence of hydrate formation in the equilibrations carried out at higher CO_2 pressures. The data collected at 400, 600, and 800 psig all fall within the expected range of hydrate formation (refer to Figure 5), and this would decrease the amount of dissolved CO_2 detected in the water phase, thus lowering the CO_2 Fermi dyad peak areas relative to the calculated CO_2 concentration.

Though not enough data points were collected to confirm or reject this hypothesis, it is one possible explanation for the increased error in that set.

CONCLUSIONS/RECOMMENDATIONS

In summary, a thorough comparison of the Brewer team's lab and seagoing Raman systems was carried out with the aim of optimizing plans for future in situ experiments.

The pressure of CO_2 equilibrated in seawater is related to the concentration of CO_2 gas that dissolves into the seawater through a modified Henry's law equation; the dissolved gas concentration, in turn, is directly related to the summed and normalized Raman peak areas of the CO_2 Fermi dyad.

The two Raman systems were compared through a series of spectral collections of solutions containing known concentrations of sodium sulfate and through these experiments, an average sensitivity ratio of 3.1:1 was calculated for the DORISS II: laboratory Raman instrument. This establishes a method for translating the results from one system to make a prediction of raw results for the other system when measuring chemical composition under the same conditions.

And finally, the CO_2 detection limit for the DORISS II system was estimated around 7-8 mM. This is an improvement on the previous estimate made by Dunk et al. in 2005 and indicates that the study of natural oxidation processes occurring in marine sediments through CO_2 pore water measurements should be feasible, provided that a reliable phosphoric acid delivery system is developed.

A few key issues will need to be resolved in order to successfully carry out the CO_2 pore water studies. First, improved spectral processing techniques, particularly for the baseline correction step, will make the detection of significant spectral peaks easier and more consistent. The primary tool we have been developing for this is a MATLAB program that would make the corrections automatically.

Baseline noise could also be reduced through the incorporation of a more powerful laser into the DORISS II system; this would have the added bonus of lowering the detection limit for CO_2, which would enable us to carry out even more investigations

on the environment of the sub-seafloor and its capabilities for greenhouse gas sequestration.

And finally, the implementation of an acid delivery system to make all dissolved inorganic carbon measureable using our Raman system is necessary for any experiments to be successfully carried out. An initial version of this system is already in place and will be tested in situ in the near future.

ACKNOWLEDGEMENTS

First and foremost, I would like to acknowledge the entire Brewer team. Peter Brewer, Ed Peltzer, and Peter Walz have provided me with endless help, guidance, and knowledge throughout the internship; I feel privileged to have had the opportunity to work with all of them. It has been a pleasure working at MBARI and I am grateful to the entire staff for welcoming me as well as to the David and Lucile Packard Foundation for funding my ten weeks of research. And last, but not least, I would like to recognize George Matsumoto and Linda Kuhnz for organizing the summer intern program and providing me with the chance to learn, explore, and grow as a scientist.

References:

Benedict, M., Webb, G.B., and Rubin, L.C. (1940). An Empirical Equation for Thermodynamic Properties of Light Hydrocarbons and Their Mixtures I. Methane, Ethane, Propane, and n-Butane. *Journal of Chemical Physics*, 8: 334-345.

Benedict, M., Webb, G.B., and Rubin, L.C. (1942). An Empirical Equation for Thermodynamic Properties of Light Hydrocarbons and Their Mixtures II. Mixtures of Methane, Ethane, Propane, and n-Butane. *Journal of Chemical Physics*, 10: 747-758.
Brewer, P.G., Malby, G., Pasteris, J.D., White, S.N., Peltzer, E.T., Wopenka, B., Freeman, J., Brown, M.O. (2004). Development of a laser Raman spectrometer for deep-ocean science. *Deep-Sea Research I*, 51:739-753.

Brewer, P.G. (2007). Evaluating a technological fix for climate. *Proceedings of the National Academy of Sciences*, 104, 9915-9916.

Carey, D.M., and Korenowski, G.M. (1998). Measurement of the Raman spectrum of liquid water. *Journal of Chemical Physics*, 108(7): 2669-2675.

Cherif, M., Mgaidi, A., Ammar, N., Vallée, G., and Fürst, W. (2000). A New

Investigation of Aqueous Orthophosphoric Acid Speciation Using Raman Spectroscopy. *Journal of Solution Chemistry*, 29(3): 255-269.

Coward, E. (2011). Rates of CH_4 Displacement by a N_2-CO_2 Mixture in CH_4 Hydrates. In: *2011 Intern Papers, Monterey Bay Aquarium Research Institute*, http://www.mbari.org/education/internship/11interns/papers/2011_papers.html.

Davis, A.R. and Oliver, B.G. (1972). A Vibrational-Spectroscopic Study of the Species Present in the CO_2-H_2O System. *Journal of Solution Chemistry*, 1(4): 329-339.

Dunk, R.M., Peltzer, E.T., Walz, P.M., and Brewer, P.G. (2005). Seeing a Deep Ocean CO_2 Enrichment Experiment in a New Light: Laser Raman Detection of Dissolved CO_2 in Seawater. *Environmental Science and Technology*, 39(24): 9630-9636.

Fröelich, P.N., Klinkhammer, G.P., Bender, M.L., Luedtke, N.A., Heath, G.R., Cullen, D., and Dauphin, P. (1979). Early oxidation of organic matter in pelagic sediments of the eastern equatorial Atlantic: suboxic diagenesis. *Geochimica et Cosmochimica Acta*, 43(7): 1075:1090.

Hofmann, A.F., Peltzer, E.T., and Brewer, P.G. (2012). Gas exchange rates for animals in the deep-sea II: Carbon Dioxide. *Global Biogeochemical Cycles*, Submitted.

Johansen, O., Rye, H., and Cooper, C. DeepSpill (2003). Field Study of a Simulated Oil and Gas Blowout in Deep Water. *Spill Science & Technology Bulletin*, 8:433-443.

Knopf, D.A., Luo, B.P., Krieger, U.K., and Koop, T. (2003). Thermodynamic Dissociation Constant of the Bisulfate Ion from Raman and Ion Interaction Modeling Studies of Aqueous Sulfuric Acid at Low Temperatures. *Journal of Physical Chemistry*, 107: 4322-4332.

McCreery, R.L. (2000). Raman Spectroscopy for Chemical Analysis. Volume 157 in: (J.D. Winefordner, ed.) *Chemical Analysis*. Wiley-Interscience, New York.

Paull, C.K., Ussler, W., Peltzer, E.T., Brewer, P.G., Keaten, R., Mitts, P.J., Nealon, J.W., Gerinert, J., Herguera, J., and Perez, M.E. (2007). Authigenic carbon entombed in methane-soaked sediments from the northeastern transform margin of the Guaymas Basin, Gulf of California. *Deep-Sea Research Part II*, 54: 1240-1267.

Reeburgh, W.S. (2007). Oceanic methane biogeochemistry. *Chemical Reviews*, 107: 486-513.

Rehder, G., Kirby, S.H., Durham, W.B., Stern, L.A., Peltzer, E.T., Pinkston, J., and Brewer, P.G. (2004). Dissolution rates of pure methane hydrate and carbon-dioxide hydrate in undersaturated seawater at 1000-m depth. *Geochimica et Cosmochimica Acta*, 68(2): 285-292.

Riestenberg, D.E., Tsouris, C., Brewer, P.G., Peltzer, E.T., Walz, P.M., Chow, A.C., and Adams, E.E. (2005). Field Studies on the Formation of Sinking CO_2 Particles for Ocean Carbon Sequestration: Effects of Injector Geometry on Particle Density and Dissolution Rate and Model Simulation of Plume Behavior. *Environmental Science and Technology*, 39(18): 7287-7293.

Rudolph, W.W. and Irmer, G. (2011). Vibrational spectroscopic studies and DFT calculations on tribromoacetate and tribromoacetic acid in aqueous solution. *Spectrochimica Acta Part A: Molecular and Biomolecular Spectroscopy*, 79(5): 1483-1492.

Thistle, D., Sedlacek L., Carman K.R., Fleeger, J.W., Brewer, P.G., and Barry, J.P. (2007). Exposure to carbon dioxide-rich seawater is stressful for some deep-sea species: an in situ, behavorial study. *Marine Ecology Progress Series*, 340: 9-16.

Weiss, R.F. (1974). Carbon dioxide in water and seawater: the solubility of a non-ideal gas. *Marine Chemistry*, 2(3): 203-215.

Zeebe, R.E. and Wolf-Gladrow, D. (2001). *CO_2 in Seawater: Equilibrium, Kinetics, Isotopes*, no. 65 in Elsevier Oceanography Series, first ed., Elsevier.

Zhang, X., Walz, P.M., Kirkwood, W.J., Hester, K.C., Ussler, W., Peltzer, E.T., and Brewer, P.G. (2010). Development and deployment of a deep-sea Raman probe for measurement of pore water geochemistry. *Deep-Sea Research I*, 57: 297-306.

Zhang, X., Hester, K.C., Ussler, W., Walz, P.M., Peltzer, E.T., and Brewer, P.G. (2011). In situ Raman-based measurements of high dissolved methane concentrations in hydrate-rich ocean sediments. Geophysical Research Letters, 38: L08605.

Zhang, X., Kirkwood, W.J., Walz, P.M., Peltzer, E.T., and Brewer, P.G. (2012). A Review of Advances in Deep-Ocean Raman Spectroscopy. *Applied Spectroscopy*, 66(3): 237-249.